J. Plasma Physics (1969), *vol.* 3, *part* 3, *pp.* 449–463
Printed in Great Britain

MHD Rankine–Hugoniot equations applied to earth's bow shock

By J. D. MIHALOV, C. P. SONETT AND J. H. WOLFE

Space Sciences Division, Ames Research Center, NASA,
Moffett Field, California 94035, USA

(Received 14 February 1969 and in revised form 14 April 1969)

This paper compares computed results with upstream and downstream thermal pressures, and the downstream ion density and vector flow velocity measured by the Ames plasma probe on the Pioneer 6 spacecraft as earth's bow shock was traversed. The upstream ion density and vector flow velocity measured on Pioneer 6 by this experiment are used as independent variables, together with Pioneer 6 magnetic field measurements. MHD Rankine–Hugoniot equations for an isotropic plasma are used for these computations. Reasonable agreement is obtained between the measured and computed downstream ion density, thermal pressure and convective velocity magnitude and orientation, only when a 1γ change is made to a downstream magnetic field value used in the calculation. There is disagreement between several determinations of shock orientation and that deduced from coplanarity of the reported magnetic fields, and the shock orientation provides the co-ordinate system for solving the Rankine–Hugoniot equations. If a shock orientation determined by velocity coplanarity is used in the calculations, all computed quantities agree well with the experimental results. Other results suggest that a disagreement between computed and measured upstream thermal pressures may not be negligible in comparison with experimental uncertainties in upstream velocity and density. If the computations included anisotropic pressure terms and/or other factors such as plasma turbulence, better agreement might be obtained between computed and measured upstream thermal pressures.

1. Introduction

The existence of extraterrestrial shock waves in collision-free plasmas rests upon the hypothesis of the propagation of disturbances from the sun to earth (Gold 1955), observation of the storm events of March–April 1960 on Pioneer 5 (Coleman, Sonett & Davis 1961; Greenstadt & Moreton 1962), observation and analysis of the storm of 7 October 1962, seen by Mariner 2 (Sonett, Colburn, Davis, Smith & Coleman 1964; Wolfe & Silva 1965), study of SI^+–SI^- pairs in ground magnetic records (Sonett & Colburn 1965; Razdan, Colburn & Sonett

1965), and extensive observations of earth's bow wave initiated by Explorer 18 (Ness, Scearce & Seek 1964; Bridge, Egidi, Lazarus, Lyon & Jacobson 1965; Wolfe, Silva & Myers 1966) and the Vela 2 satellites (Gosling, Asbridge, Bame & Strong 1967). Recent review articles (Wilcox 1968; Spreiter, Alksne & Summers 1968) summarize a considerable number of later observations (Heppner, Sugiura, Skillman, Ledley & Campbell 1967). For some of the observations, rather complete plasma jump data are available, and in the case of the Mariner observations (Sonett *et al.* 1964) a test using the MHD Rankine–Hugoniot equations has been presented. General consistency was obtained from computer matching of the over-determined problem and agreement was found between some computed and measured properties of the shock, such as the preshock and post-shock Mach numbers and the temperature, and the radial component of velocity. However, the fit was not satisfactory in all aspects. In particular, the interplanetary event whose leading edge defined the shock is thought to have been recurrent. This suggests that the unit normal to the shock wave should make a large angle with the outward pointing vector from the sun. However, the unit normal was nearly in the direction of the outward pointing vector from the sun.

This paper presents an extension of the analysis applied to the Mariner observations (Sonett *et al.* 1964) to earth's bow wave. Certain characteristics of the present problem are more refined due to the more sophisticated measurements which are made. In particular, the vector bulk plasma velocity is available both upstream and downstream from the shock. Pioneer 6 measurements provide both the plasma speed and the two angular components of the flow. Also, the geometry is considerably different here; the shock wave is nearly fixed in the co-ordinate system of the spacecraft, and the Mach number is high (i.e. the shock is a standing wave before the magnetosphere rather than propagating in the interplanetary stream). The standing shock we investigate is observed under some of the quietest geomagnetic conditions for which spacecraft data are available.

Computer calculations are presented for which certain dependent variables are matched to measured parameters. The calculations are basically fluid dynamical in nature. They exclude considerations of viscosity, electrical resistance, thermal conductivity or certain other processes which might be considered in a microscopic description. Essentially we seek a match between a fluid description and the measured jump parameters across the shock wave. The quality of the fit determines to some extent the applicability of the concept of a MHD shock wave in the collision-free limit. Some significant tests are correct values for the jumps in the plasma parameters (Sonett *et al.* 1964; see also Spreiter, Summers & Alksne 1968 and Burlaga & Ogilvie 1968), subunity Mach numbers for the post-shock flow normal to the shock, and evidence that momentum flux is conserved across the shock jump by virtue of correctness of velocity and magnetic field coplanarity. A discussion of the structure of the leading edge of the shock jump must be regarded as speculative since the data are subject to signal distortion from a variety of effects. Whether these effects are important and will modify speculations regarding the structure of the leading edge must await the publication of higher frequency magnetic field data from Pioneer 6.

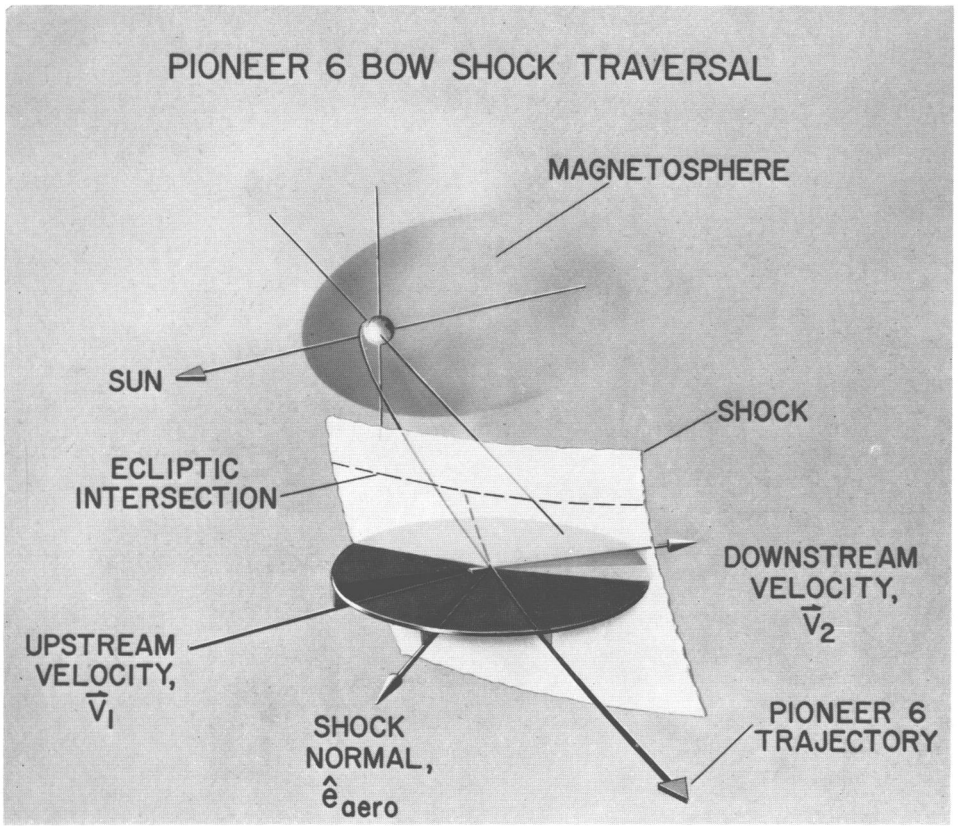

FIGURE 1. Pictorial representation of the Pioneer 6 bow shock traversal. The spacecraft passes southward through the bow shock at a point south of the ecliptic plane and slightly forward of the dusk meridian plane. The grey disk with centre at the traversal point is parallel to the ecliptic plane, demonstrating that the observed upstream and downstream plasma flows, $\mathbf{V}_1$ and $\mathbf{V}_2$, were slightly northward, and the shock normal, $\hat{\mathbf{e}}_{aero}$, computed assuming velocity coplanarity, is tipped slightly southward.

2. Geometry and orbit

The Pioneer 6 spacecraft was launched on 16 December 1965. The experiments providing data for the present discussion are the Ames quadrispherical plasma probe (Wolfe, Silva, McKibbin & Mason 1966) and the magnetometer (Ness, Scearce & Cantarano 1966). The launch resulted in a magnetospheric trajectory generally in the afternoon hemisphere. Exit of the spacecraft from the magnetosphere took place at 1256 UT and transit through the shock front was at 1712 UT, some 4 h and 16 min later. The bow shock was observed at a geocentric distance of 20·4 earth radii, and at $-81{\cdot}25°$ longitude and $-4{\cdot}4°$ latitude in an earth-centred, solar-oriented ecliptic co-ordinate system. Here positive longitude is measured

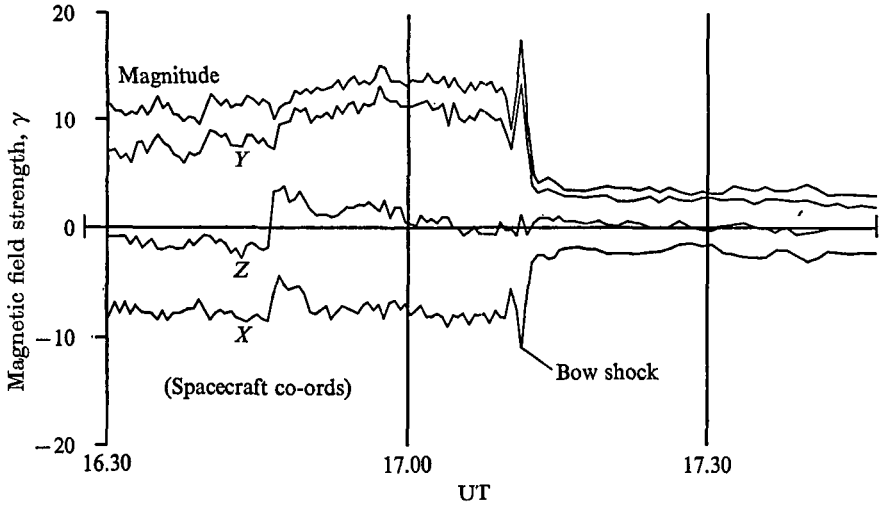

FIGURE 2. Pioneer 6, 30-second averages of magnetic field data (Ness, Scearce & Cantarano 1966) during the traversal of earth's bow shock, presented in a 'spacecraft' co-ordinate system, defined in the text.

from the solar direction toward the direction of planetary motion and positive latitude is measured northward from the solar direction. The trajectory of the spacecraft traverses post-shock (downstream) gas first. Identification of the passage of the spacecraft through the magnetopause and the shock is made jointly from the plasma and magnetometer data; plasma data display the onset of transition region flow and both instruments indicate the terminus of the post-shock flow and exit into the free-stream solar wind (Wolfe & McKibbin 1968).

The measured plasma velocities, both in the free stream and in the transition region during the traversal, are as low as ever measured in these regions. Also, the flow was exceptionally steady during transit through the magnetosheath and on into the solar wind. Confirmation of the very quiet conditions is given by the low Ap value of 1 during the time of interest (Lincoln 1966). The geometry of the trajectory and other pertinent information are shown schematically in figure 1.

The final orientation of the Pioneer spacecraft is with the spin axis directed toward the south ecliptic pole. The two remaining manoeuvres which completed spacecraft orientation had not been performed before passage through the

magnetosheath, during which the spin axis direction is tipped 1·6° toward the sun out of a plane normal to the solar direction, and canted at an angle of 38° to the south ecliptic pole, in the direction opposite to earth's motion. Although certain magnetometer data in this paper, including figures 2 and 3, are presented in a 'spacecraft' co-ordinate system (defined in the next section), most of the plasma and magnetometer data are presented in an ecliptic co-ordinate system. In each case, the co-ordinate system in which the data are presented is indicated.

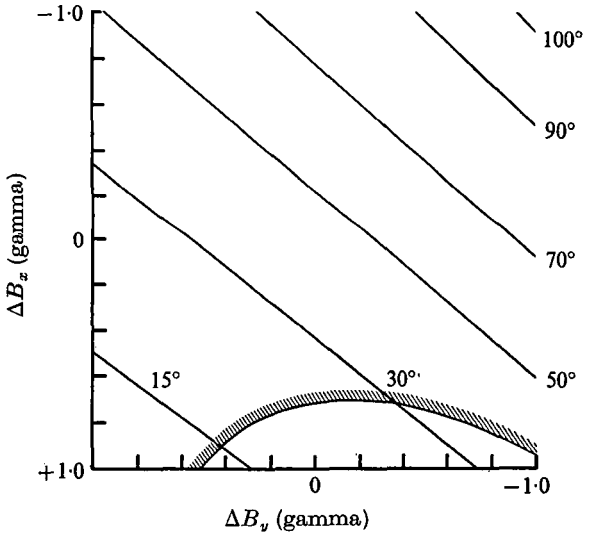

FIGURE 3. Effect of 'biases' to the measured post-shock magnetic fields on the angle between two computed shock normals, one which assumes coplanarity of measured plasma velocities (see text) and the other which assumes magnetic field coplanarity. The 'biases', ΔB_x and ΔB_y, are applied to the measured 'spacecraft' co-ordinate x- and y-component magnetic fields. No 'bias' is applied to measured z-component magnetic fields. Field variations above, or to the shaded side of a line which crosses the plot result in negative computed upstream thermal pressures.

The ecliptic co-ordinate system used here is an orthogonal, right-handed heliocentric co-ordinate system (RTN) defined with $+R$ in the antisolar direction and $+N$ northward and perpendicular to the ecliptic plane. The 1·6° tilt described above is ignored.

3. Data

The plasma probe measures the flux and energy (per unit charge) of ions in 120 different directions. Solar wind speeds, flow directions, temperatures and densities are derived from the measured fluxes. Some analysis of the Pioneer 6 near-earth plasma observations has appeared (Wolfe & McKibbin 1968; Spreiter & Alksne 1968). A subsequent more refined analysis of the data obtained near the bow shock traversal, using an instrument simulation computer program, has produced the values of vector convective or bulk plasma velocities used in this paper. The instrument simulation program mathematically models the plasma

probe and produces best-fit parameters for a bi-Maxwellian model (Wolfe, Silva, McKibbin & Mason 1966) of the interplanetary and shocked plasma. The plasma parameters are obtained from repetitive trial fits to obtain the plasma parameters of the bi-Maxwellian model to which the observed fluxes are most closely matched. These plasma parameters which are used in the calculations are shown in Table 1. The ion velocity distributions observed in the magnetosheath are strongly non-Maxwellian, compared with the free stream (Wolfe & McKibbin

Parameter	Interplanetary	Magnetosheath
Bulk velocity, km s^{-1}	280 ± 30	180 ± 20
ϕ ('spacecraft' co-ordinates), deg	$9{\cdot}9 \pm 1$	$30{\cdot}4 \pm 4$
θ ('spacecraft' co-ordinates), deg	$2{\cdot}2 \pm 1$	$21{\cdot}1 \pm 4$
Ion density, cm^{-3}	11 ± 3	31 ± 8
Ion temperature, °K	3×10^4 °K (mean)	$5{\cdot}0$–$7{\cdot}5 \times 10^5$ °K (thermal part)
Electron temperature, °K	2×10^5 °K	5×10^5 °K
Magnetic field strength, γ	3·5	13·1
R-component	+2·3	+8·2
T-component	−2·0	−8·3
N-component	+1·8	+6·1

TABLE 1. Measured plasma and magnetic field parameters adjacent to bow shock—Pioneer VI

1968). This precludes a precise definition of magnetosheath ion temperatures. Uncertainties in electron temperatures are affected by vehicle surface potential configurations. Using a bi-Maxwellian model, the upstream ion velocity is anisotropic, with $T_\perp \sim 4 \times 10^4$ °K, $T_\parallel \sim 1 \times 10^4$ °K and $T_\parallel/T_\perp \sim 0{\cdot}25$ (Wolfe & McKibbin 1968). The flow vector orientation angles are defined in 'spacecraft' co-ordinates with ϕ measured clockwise in the spacecraft equatorial plane from the antisolar direction when viewed from the north, and θ measured positive northward and perpendicular to the spacecraft equatorial plane.

Magnetometer data (Ness *et al.* 1966) are given in figure 2 in the 'spacecraft' co-ordinate system. The X-axis of the system is in the solar direction, the Z-axis is in the opposite direction from the spacecraft angular momentum vector, and the Y-axis completes an orthogonal, right-handed co-ordinate system, XYZ. After the spacecraft spin axis is rotated to its final position directed toward the south ecliptic pole, positive directions along the two axes of the 'spacecraft' co-ordinate system in the ecliptic plane are at 180° to the $+R$ and $+T$ axes. The data points indicated on figure 2 each represent a 30-second average of magnetic field component measurements.

For computations, 12 post-shock 30-second averages and all 35 interplanetary averages reported by Ness *et al* (1966) are resolved into components in the 'spacecraft' co-ordinate system, averaged, and then transformed to ecliptic co-ordinates to obtain values presented in Table 1. The onset pulse at the leading edge of the shock structure which was predicted from theory (Davis, Lüst & Schlüter 1958) is treated separately. For the jump calculations, these 5 data

points, representing 150 seconds, are not included in the averages used because the onset pulse is not typical of mean values observed on either side of the jump. The transformed data points include a reasonable sample to either side of the shock jump, without inclusion of extreme values which occurred further into the post-shock flow.

4. Shock jump conditions

Of the eight conservation equations specifying the MHD generalization of the jump relations (De Hoffmann & Teller 1950), a reduction to five is made directly by rotation of the co-ordinates so that one axis is normal to the plane of the shock, and a second is aligned along the tangential component of the magnetic field (see Colburn & Sonett 1966 or Helfer 1953). We follow the procedure adopted in the earlier calculation (Sonett *et al.* 1964; Colburn & Sonett 1966) and regard the upstream and downstream magnetic fields and upstream density and velocity as independent variables, and the ratio of specific heats as constant. We solve for both upstream and downstream thermal pressures, $nk(T_i+T_e)$, and the downstream density and velocity. Here n is the ion density, T_i and T_e are ion and electron temperatures and k is Boltzmann's constant. The calculations are performed in a co-ordinate system defined by a shock orientation which assumes magnetic field coplanarity on either side of the shock (Colburn & Sonett 1966). This shock orientation is also compared with orientations which assume velocity coplanarity or an aerodynamic approximation. The solutions are more complete than in the earlier case since all components of the bulk velocities are known here. Ion and electron contributions are accounted for in the calculation using total thermal pressure terms, $p = nk(T_e+T_i)$, in the energy and normal momentum flux conservation equations. Also, the equation of state admitted in these calculations is assumed invariant to passage of the gas through the shock front. The same equation of state is assumed for both ions and electrons. The following equations are solved.

$$[\rho v_\gamma] = 0,$$

$$\left[\rho v_\gamma^2 + p + \frac{B_\beta^2}{2\mu_0}\right] = 0,$$

$$\left[\rho v_\gamma v_\beta - \frac{B_\gamma B_\beta}{\mu_0}\right] = 0,$$

$$\left[\frac{v^2}{2} + \frac{\gamma}{\gamma-1}\frac{p}{\rho} + \frac{v_\gamma B_\beta^2 - v_\beta B_\beta B_\gamma}{\rho v_\gamma \mu_0}\right] = 0,$$

$$[v_\gamma B_\beta - v_\beta B_\gamma] = 0.$$

Here ρ, v and $\mathbf{B}$ represent the gas density and components of the flow velocity and magnetic field, respectively. $[A] = A_2 - A_1$ where the subscripts 1 and 2 refer to preshock and post-shock quantities, respectively; α, β and γ refer to three orthogonal directions forming a right-handed system such that γ is the direction normal to the shock, and the magnetic field in the shock plane is in the β direction. $B_{1\gamma} = B_{2\gamma}$, invoking the nondivergence of $\mathbf{B}$.

The plasma and magnetic field data for the entire Pioneer 6 magnetosheath traversal previously also have been compared with theoretical estimates of plasma velocity, ion density and magnetic field strength derived from a continuum fluid model of the steady-state interaction (Spreiter & Alksne 1968; Spreiter *et al.* 1968). Exact MHD solutions as used in this paper are available along the shock surface and along the stagnation streamline, and have been compared with results using the continuum fluid model for bow shocks (Alksne 1967) with good agreement except for a restricted range of shock and magnetic field

Parameter	Measured	Computed	Magnetic bias	Velocity coplanarity
Interplanetary				
Thermal pressure, dynes cm^{-2}	$3{\cdot}5 \pm 0{\cdot}9 \times 10^{-10}$	$-6{\cdot}3 \times 10^{-11}$	$3{\cdot}8 \times 10^{-11}$	$2{\cdot}8 \times 10^{-10}$
Magnetosheath				
Thermal pressure, dynes cm^{-2}	$5{\cdot}4 \pm 1{\cdot}4 \times 10^{-9}$	$5{\cdot}9 \times 10^{-10}$	$3{\cdot}7 \times 10^{-9}$	$6{\cdot}6 \times 10^{-9}$
Ion density, cm^{-3}	31 ± 8	41	40	37
Convective velocity magnitude, $km\,s^{-1}$	180 ± 20	261	212	164
R-component	158 ± 11	257	196	145
T-component	-89 ± 14	-42	-80	-75
N-component	2 ± 18	20	-13	7

TABLE 2. Results of Rankine–Hugoniot equation calculations

orientations. Here we present a correspondence of experimental results for undisturbed interplanetary conditions with exact MHD solutions and discuss further the shock orientation.

5. Results from MHD Rankine–Hugoniot equations

Table 2 compares with the measured values of Table 1 the thermal pressures upstream and downstream from the shock, and the downstream ion density and vector velocity, computed from the Rankine–Hugoniot equations given above. The first column gives the experimental results; the second column gives computed results for an assumed ratio of specific heats for a monatomic gas with only three degrees of freedom, $\gamma = \frac{5}{3}$. There is reasonable agreement only between computed and measured values of downstream ion density and the N-component of convective velocity magnitude. Other disagreements between computed and measured quantities are discussed extensively in the next two sections. The remaining two columns of Table 2 are results from these studies.

6. Modifications and possible refinements of the calculation

The magnetic field values used in the calculations are averages of vector quantities derived from averages of measurements of orthogonal components of the magnetic field (Ness *et al.* 1966). Correct values to use in the Rankine–

Hugoniot equations may be masked by the component averaging procedure which was used first. Thirty-percent uncertainties in hourly average Pioneer 6 magnetic field magnitudes due to this averaging procedure are sometimes noted (Ness & Taylor 1967). Also, the rms deviation in a component of post-shock magnetic field is about 3γ (Ness *et al.* 1966). Consequently, the rms deviation in the magnetic field magnitude may be estimated at 5γ or 40 %. Publication of higher frequency magnetic field data from Pioneer 6 would clarify this point.

A possible additional source of error in the magnetic field values used in the calculations arises from the nonsimultaneous sampling procedure of the Pioneer 6 magnetometer (Ness *et al.* 1966). It is clear that an ambient magnetic field which fluctuates rapidly during the time for one revolution of the spacecraft cannot be correctly reconstructed when the three components of the vector magnetic field are not sampled simultaneously. Possibly additional error in reported downstream magnetic fields then arises from this source, considering the high level of field fluctuations reported.

The sensitivity of the computed results of Table 2 to variations in downstream magnetic field has been studied. The shock calculations have been repeated with arbitrary, systematic variations, to $\pm 1\gamma$ in each of two components perpendicular to the spacecraft spin axis, of the reported magnetic field downstream from the shock. The third column of Table 2 gives the computed results for the best values of downstream magnetic field 'bias' in this range, $\Delta B_x = +1\gamma$, $\Delta B_y = \Delta B_z = 0$ in 'spacecraft' co-ordinates. These results show a spectacular improvement in agreement of computed and measured downstream thermal pressure and convective velocity magnitude and orientation. Absolute trust in the reported magnetic field results has been discarded. It appears likely that sources of error which have been discussed contaminate the reported magnetic field values to some extent. A further discussion of effects on these calculations of 'biasing' downstream magnetic fields appears in the next section.

The computed negative value of upstream thermal pressure in column 2 of Table 2 is now discussed. The negative value might not be considered significant since its magnitude is only 1 % of the upstream convective pressure compared with the ± 27 % experimental uncertainties in the upstream convective pressure. However, negative values are also always obtained if the calculation of upstream thermal pressure is done using as independent variables different values for upstream convective pressure throughout the range of the experimental uncertainties. Consequently, in this case there is no evidence for a direct effect on the sign of the computed upstream thermal pressure due to experimental uncertainties in the upstream convective pressure.

The computed upstream thermal pressure becomes positive when the value of the ratio of the specific heats, γ, used in this calculation is lowered by 10 % to $\gamma = 1{\cdot}5$, while the other quantities of Table 2 are unchanged except for a 10 % increase in the downstream thermal pressure. A physically realistic procedure might be decreasing γ only downstream from the shock. This procedure also might produce agreement between measured and computed thermal pressures, but cannot be done with the present computer routine. This procedure would be equivalent from the viewpoint of kinetic theory to introducing a larger number

of degrees of freedom for the post-shock gas. Abraham-Shrauner (1968) introduces into the conservation equations terms representing effects of plasma turbulence. If such terms were included in the above solution, the effect could be identical to that when γ is lowered. Detailed consideration of these plasma turbulence terms is impossible in this case because of the lack of electric field strength measurements. However, the available Pioneer 6 data do suggest the presence of turbulence behind the bow shock (Wolfe & McKibbin 1968). Including plasma anisotropy in the shock jump conditions (Abraham-Shrauner 1967) might also produce agreement between computed and measured thermal pressures. It is beyond the scope of this paper to estimate whether a significant added contribution to the conservation equations for the case considered arises from plasma anisotropy, turbulence or some other effect alone.

7. Shock orientations

In assessing the direction of the shock normal, we have invoked the coplanarity of the upstream and downstream magnetic fields (Colburn & Sonett 1966). For the strong shock approximation, a reasonable alternate assumption is that the jump in velocity is primarily along the normal to the shock face ('velocity coplanarity'). This assumes that the effect of the magnetic field is negligible. Then the outward unit normal to the shock, $\hat{\mathbf{i}}_s \simeq \Delta\mathbf{V}/|\Delta\mathbf{V}|$, where $\Delta\mathbf{V} = \mathbf{V}_2 - \mathbf{V}_1$. A third determination considers the unit normal from the continuum fluid model (Spreiter, Summers & Alksne 1966). In this method the entire shock shape is calculated and the unit normal used is that at the point where the shock is crossed. This method is approximately valid here to the extent that the convective energy density incident upon the bow shock exceeds the magnetic field energy. In the present case, $(\frac{1}{2}nmv^2)/(B_1^2/2\mu_0) \cong 150$, where m is the mean mass of solar wind ions, v is the convective velocity and B_1 is the magnetic field strength. The above ratio is approximately 12 behind this shock. Furthermore, in this case the true shock orientation is expected to differ by $\lesssim 2°$ from the velocity coplanarity orientation. This estimate is made by comparing the change in downstream flow orientation computed from the mass flux and tangential momentum flux conservation equations, from the flow orientation computed with the magnetic fields ignored. This estimate basically uses the continuum fluid model shock orientation for obtaining normal components of flow velocity, and does not assume a magnetic coplanarity shock orientation.

Table 3 compares the shock normal direction cosines according to the continuum fluid model, velocity coplanarity, magnetic coplanarity and the varied magnetic coplanarity corresponding to the best field bias introduced for the jump calculations. Lastly, the upstream velocity is varied within the limits of the experimental uncertainties to an extreme value which, however, preserves the agreement between measured and computed shock jump parameters of Table 2. Also, Table 3 gives in parentheses the angles between the positive *RTN* axes and the various shock normals. The continuum fluid result (Spreiter, Summers & Alksne 1966) corresponds to $\gamma = \frac{5}{3}$ and $M_\infty = v(2\gamma RT)^{-\frac{1}{2}} = 8$, the upstream sonic Mach number, and includes the measured aberration of the upstream flow; R is

the gas constant, T is a measure of gas internal energy and the mean molecular weight has been taken as $\frac{1}{2}$. The continuum fluid model shock orientation agrees fairly well with the velocity coplanarity and varied magnetic coplanarity orientations, but less well with that deduced using coplanarity of the reported magnetic fields for which the normal is tipped about 30° out of the ecliptic plane away from the other normals. Table 3 shows that upstream velocity uncertainties do not cause appreciable uncertainties in velocity coplanarity shock orientation.

Component	Continuum fluid model	Velocity coplanarity		Magnetic coplanarity	
		Measured	Biased	Biased	Measured
R	−0·656 (131°)	−0·860 (149°)	−0·909 (156°)	−0·663 (132°)	−0·349 (110°)
T	−0·751 (139°)	−0·491 (119°)	−0·396 (113°)	−0·697 (134°)	−0·726 (136°)
N	−0·077 (94°)	−0·140 (98°)	−0·134 (98°)	−0·273 (106°)	−0·593 (126°)

TABLE 3. Calculated and measured values of the outward unit normal to the shock plane

Figure 3 shows the effect of 'biases' to the measured post-shock magnetic fields on the angle between two computed shock normals, one which assumes velocity coplanarity and the other which assumes magnetic field coplanarity. Previously it was estimated that the true shock orientation is expected to differ by $\lesssim 2°$ from the velocity coplanarity orientation in this case. However, the choice of 1γ 'biases' in the spacecraft equatorial plane produces agreement of the two normals only to within 9°. The results which lead to figure 3 demonstrate that more than 1γ 'biases' to both the X and Y components ('spacecraft' co-ordinates) of the reported downstream magnetic fields would be necessary for agreement of the velocity and magnetic coplanarity shock orientations to as close as 2°. Figure 3 also shows which 'biases' result in negative computed upstream thermal pressures, namely, those above, or to the shaded side of a line which crosses the plot.

These calculations have been extended to values of magnetic field variation, or 'bias', for which the magnetic field coplanarity shock orientation agrees with the velocity coplanarity shock orientation. The resulting solutions of the MHD Rankine–Hugoniot equations are those obtained if the shock orientation is correctly given by velocity coplanarity. The fourth column of Table 2 gives results of these extended calculations, and excellent agreement of all computed quantities with experimental values is obtained. These computed values are obtained with $\Delta B_x = +2{\cdot}6\gamma$, $\Delta B_y = -0{\cdot}4\gamma$ and $\Delta B_z = 0$ in 'spacecraft' co-ordinates.

Magnetic field variations other than those described above, such as variations of the Z component and upstream reported magnetic fields in various combinations, are of course possible. Studies of these variations are not reported here.*

* *Note added in proof.* Variations of the downstream Z component ('spacecraft' co-ordinates) have been performed but these do not improve the match of magnetic field coplanarity and velocity coplanarity results which is reported.

8. Mach numbers

A fundamental test for a shock hypothesis is that the downstream Mach number in the direction normal to the shock be less than unity. The observed characteristic velocities and Mach numbers are presented in Table 4. The maximum ion temperature has been used to calculate the upstream disturbance velocities in the flow direction, given in the upper part of Table 4. The fast and slow wave velocities (Jeffrey & Taniuti 1964) in the flow direction are also given in the upper part of Table 4. The fast and slow mode Mach numbers normal to the shock front, given in the two lower parts of Table 4, were calculated using flow

	Interplanetary space (upstream)	Magnetosheath (downstream)
Bulk velocity, km s^{-1}	280 ± 30	180 ± 20
Sonic velocity, km s^{-1}	33	~ 140
Sonic Mach number	8·4	$\sim 1{\cdot}3$
Alfvén velocity, km s^{-1}	23	52
Alfvén Mach number	12	3·5
Fast and slow wave velocities, km s^{-1}	38, 15	142, 43
	Values normal to the shock front	
Continuum fluid model shock orientation		
Bulk velocity, km s^{-1}	170	38
Sonic Mach number	5·1	$\sim 0{\cdot}3$
Alfvén Mach number	170	24
Fast mode Mach number	4·2	$\sim 0{\cdot}3$
Slow mode Mach number	209	25
Velocity coplanarity shock orientation		
Bulk velocity, km s^{-1}	230	91
Sonic Mach number	7·0	$\sim 0{\cdot}7$
Alfvén Mach number	29	6·1
Fast mode Mach number	5·9	$\sim 0{\cdot}6$
Slow mode Mach number	34	$\sim 6{\cdot}5$

TABLE 4. Flow characteristic velocities and Mach numbers

velocities and fast and slow wave velocities and ion temperatures normal to the shock front. The continuum fluid model shock orientation for $\gamma = \frac{5}{3}$ and $M_\infty = 8$ (Spreiter, Summers & Alksne 1966), and the velocity coplanarity shock orientation are each used separately to compute the results in the two lower parts of Table 4. The continuum fluid model orientation was used because of agreement between it and previous observations of other shock parameters (Wolfe, Silva & Myers 1966; Spreiter, Summers & Alksne 1968; Burlaga & Ogilvie 1968). The continuum fluid model and velocity coplanarity calculations did not use the same value on both sides of the shock of the component of **B** normal to the shock. The reason for this is the disagreement between these models' shock orientations and the magnetic coplanarity shock orientations; the magnetic coplanarity orientation is the only one which necessarily specifies the same normal component

of **B** on each side of the shock. Also, the upstream Alfvén and slow wave Mach numbers normal to the shock are exaggerated for the continuum fluid model orientation since the upstream magnetic field is almost tangential to this shock surface.

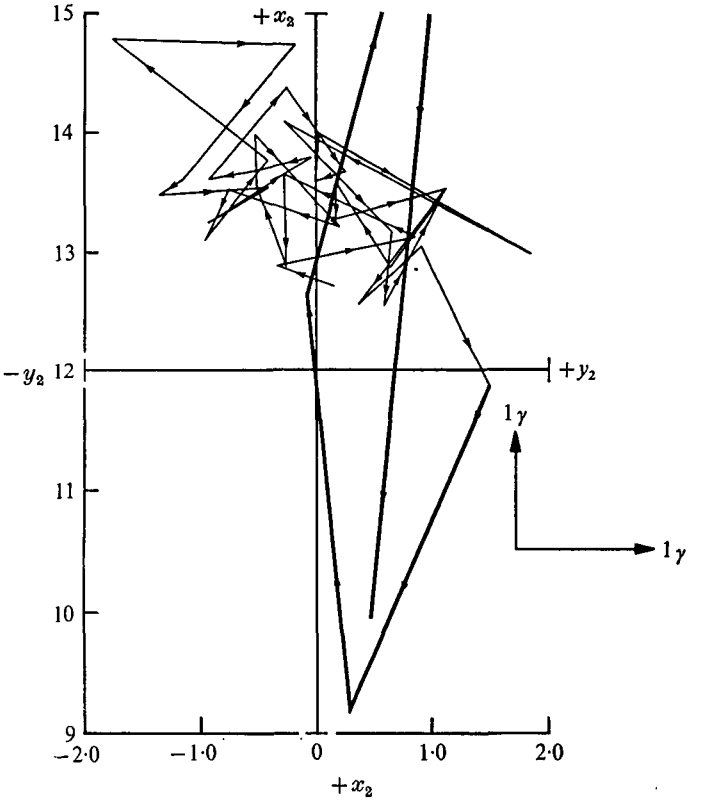

FIGURE 4. Diagram giving successive locations of heads of reported 30-second average magnetosheath magnetic field vectors (Ness *et al.* 1966). The vertical, x_2 co-ordinate is the direction of the average field in the magnetosheath alone; the y_2 co-ordinate is orthogonal to the x_2 direction and in the ecliptic plane. The data presented, from 1651 to 1712 U.T., 16 December, 1965, also include the shock transition magnetic field data, indicated by a heavier line. The arrowheads indicate directions toward later times only, and not the heads of difference vectors. Although the location of the tail of the last difference vector lies above the edge of the figure, this location is indicated by the segments of the last two difference vectors that are given on the figure.

The downstream Mach numbers for flow normal to the continuum fluid model shock are less than 1·0 for two of the four characteristic velocities, which suggests a shock hypothesis. Also, the downstream Alfvén Mach number for flow normal to the magnetic coplanarity shock exceeds 1·0, while the downstream fast mode Mach number is less than 1·0. This is the evolutionary condition satisfied by fast magnetoacoustic shocks (Jeffrey & Taniuti 1964). The sonic Mach number near 8 categorizes the shock as strong. The flow energy greatly exceeds the magnetic energy, in contrast to cases typically expected in the free-stream solar wind.

9. Pulse structure

Averages used for the shock conservation calculations excluded the 150 seconds of data which comprise the magnetic field and ion density pulse at the leading edge of the shock transition. The plasma data at the pulse have been discussed (Wolfe & McKibbin 1968). The pulse seems to display reversible properties in magnetic field strength, ion density, electron temperature and bulk flow velocity.

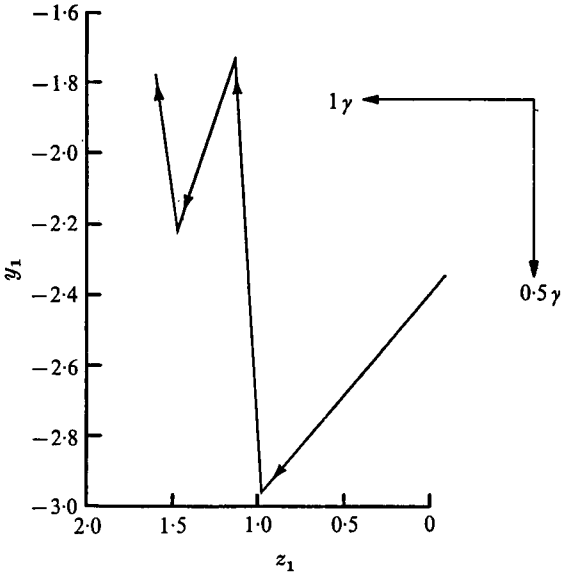

FIGURE 5. 'Head-to-tail' diagram of the reported 30-second average, shock pulse transition magnetic fields (Ness *et al.* 1966), transformed to an orthogonal, right-handed (x_1, y_1, z_1) co-ordinate system, in which the x_1 direction is that of the average preshock magnetic field and y_1 and z_1 are transverse directions with y_1 in the ecliptic plane. The first vector of the series has its origin at the origin of the co-ordinate system and is not shown. The origins of subsequent vectors are each at the head of that preceding. The arrowheads point to the origin of the following vector in the time sequence.

Attempts to disclose a non-random pattern to the polarization of the magnetic field were made. The magnetic field was resolved in a co-ordinate system defined by the average field direction. Since this direction changes through the shock wave, independent co-ordinates were defined from free stream (x_1, y_1, z_1) and post-shock (x_2, y_2, z_2) magnetic field averages. Here x_i is the average direction of the field, y_i is in the ecliptic plane and z_i completes a right-handed, orthogonal co-ordinate system. Earlier measurements of magnetosheath fields showed unmistakable evidence for elliptically polarized radiation (Siscoe, Davis, Smith, Coleman & Jones 1967; Greenstadt, Inouye, Green & Judge 1967).

Figure 4 shows the polarization of the pulse and magnetosheath magnetic field in the x_2–y_2 plane. Elliptic polarization of the field fluctuations is seen, with a ratio of axes of about 5 : 1 in the x_2–y_2 plane during the shock transition. As plotted, the field is read from the origin, i.e. difference vectors are presented. In figure 5 the 'head-to-tail' presentation of the resolution of the pulse field com-

ponents in the y_1–z_1 plane is shown. Large angular excursions in the field direction are evident through the shock pulse structure. This pulse data suggest a standing Alfvén wave pattern. A model in which the pulse structure contains a standing Alfvén wave suggests that the oscillation is large amplitude, with the first swing in field component direction being more than 90°. However, the largest field, normal to the plane of figure 5, is not shown. The time reversed transit of the pulse by the spacecraft, from the post-shock to the preshock conditions, means that the larger oscillation is to the downstream side of the shock.

10. Conclusions

The single transit of Pioneer 6 through earth's bow shock occurred during very quiet geomagnetic conditions. Using the interplanetary number density and bulk velocity vector measured by the Ames plasma probe adjacent to the shock and the magnetic field measurements on either side of the shock transition (Ness *et al.* 1966) as known quantities, the MHD Rankine–Hugoniot equations are solved. Reasonable agreement is obtained between the measured and computed downstream ion density, thermal pressure and convective velocity magnitude and orientation, only when a 1γ change is permitted in a downstream magnetic field value used in the calculation. The computed upstream thermal pressure is one-tenth the experimentally determined value, however. Disagreements between measured and computed values (see Table 2) probably are due to the use of magnetic coplanarity to establish the co-ordinate system for the shock calculations.

With regard to shock orientation, the normal derived assuming coplanarity of the measured magnetic fields is tipped about 30° out of the ecliptic plane away from shock normals derived assuming velocity coplanarity, 'biased' downstream magnetic fields or a continuum fluid model (Spreiter *et al.* 1966). When variations from the measured plasma parameters are used as independent variables in the calculation, there is not a significant improvement in the agreement of the computed with the measured quantities. However, when a shock orientation derived assuming velocity coplanarity is used, there is good agreement between all computed and measured values. The results also suggest that a disagreement between computed and measured upstream thermal pressures (see Table 2) might be due to neglect in the computations of terms such as those due to pressure anisotropy, but is not due to experimental uncertainties in the measured upstream convective pressure.

We acknowledge helpful discussions with Dr J. R. Spreiter. One of use (C. P. S.) wishes to acknowledge the aid of the Guggenheim Foundation and NASA, and the hospitality of Imperial College, London, during the final preparation of this manuscript.

REFERENCES

Abraham-Shrauner, B. 1968 *J. Geophys. Res.* **73**, 6299.

Abraham-Shrauner, B. 1967 *J. Plasma Phys.* **1**, 379.

Alksne, A. Y. 1967 *Planet. Space Sci.* **15**, 239.

BRIDGE, H., EGIDI, A., LAZARUS, A., LYON, E. & JACOBSON, L. 1965 *Space Res.* **5**, 969.

BURLAGA, L. F. & OGILVIE, K. W. 1968 *J. Geophys. Res.* **73**, 6167.

COLBURN, D. S. & SONETT, C. P. 1966 *Space Sci. Rev.* **5**, 439.

COLEMAN, P. J., Jr., SONETT, C. P. & DAVIS, L., Jr. 1961 *J. Geophys. Res.* **66**, 2043.

DAVIS, L., LÜST, R. & SCHLÜTER, A. 1958 *Z. Naturforsch.* **13a**, 916.

DE HOFFMANN, F. & TELLER, E. 1950 *Phys. Rev.* **80**, 692.

GOLD, T. 1955 Discussion in *Gas Dynamics of Cosmic Clouds*, p. 103. Amsterdam: North–Holland Publishing Co.

GOSLING, J. T., ASBRIDGE, J. R., BAME, S. J. & STRONG, I. B. 1967 *J. Geophys. Res.* **72**, 101.

GREENSTADT, E. W. & MORETON, G. E. 1962 *J. Geophys. Res.* **67**, 3299.

GREENSTADT, E. W., INOUYE, G. T., GREEN, I. M. & JUDGE, D. L. 1967 *J. Geophys. Res.* **72**, 3855.

HELFER, H. 1953 *Ap. J.* **117**, 177.

HEPPNER, J. P., SUGIURA, M., SKILLMAN, T. L., LEDLEY, B. G. & CAMPBELL, M. 1967 *J. Geophys. Res.* **72**, 5417.

JEFFREY, A. & TANIUTI, T. 1964 *Non-Linear Wave Propagation*. New York: Academic Press.

LINCOLN, J. V. 1966 *J. Geophys. Res.* **71**, 2411.

NESS, N. F. & TAYLOR, H. E. 1967 NASA Goddard Space Flight Center. Rep. No. X-612-67-345.

NESS, N. F., SCEARCE, C. S. & CANTARANO, S. 1966 *J. Geophys. Res.* **71**, 3305.

NESS, N. F., SCEARCE, C. S. & SEEK, J. B. 1964 *J. Geophys. Res.* **69**, 3531.

RAZDAN, H., COLBURN, D. S. & SONETT, C. P. 1965 *Planet. Space Sci.* **13**, 1111.

SISCOE, G. L., DAVIS, L., Jr., SMITH, E. J., COLEMAN, P. J., Jr. & JONES, D. E. 1967 *J. Geophys. Res.* **72**, 1.

SONETT, C. P. & COLBURN, D. S. 1965 *Planet. Space Sci.* **13**, 675.

SONETT, C. P., COLBURN, D. S., DAVIS, L., Jr., SMITH, E. J. & COLEMAN, P. J., Jr. 1964 *Phys. Rev. Letters* **13**, 153.

SPREITER, J. R. & ALKSNE, A. Y. 1968 *Planet. Space Sci.* **16**, 971.

SPREITER, J. R., ALKSNE, A. Y. & SUMMERS, A. L. 1968 *Physics of the Magnetosphere*, p. 301 (edited by R. L. Carovillano, J. F. McClay and H. R. Radoski). Dordrecht–Holland: D. Reidel Publishing Co.

SPREITER, J. R., SUMMERS, A. L. & ALKSNE, A. Y. 1968 *J. Geophys. Res.* **73**, 1851.

SPREITER, J. R., SUMMERS, A. L. & ALKSNE, A. Y. 1966 *Planet. Space Sci.* **14**, 223.

WILCOX, J. M. 1968 *Space Res.* **9** (in the Press).

WOLFE, J. H. & MCKIBBIN, D. D. 1968 *Planet. Space Sci.* **16**, 953.

WOLFE, J. H., SILVA, R. W., MCKIBBIN, D. D. & MASON, R. H. 1966 *J. Geophys. Res.* **71**, 3329.

WOLFE, J. H., SILVA, R. W. & MYERS, M. A. 1966 *J. Geophys. Res.* **71**, 1319.

WOLFE, J. H. & SILVA, R. W. 1965 *J. Geophys. Res.* **70**, 3575.